

Supporting Information for

Transition from vehicle to Grotthuss proton transfer in a nanosized flask: Cryogenic ion spectroscopy of protonated *p*-aminobenzoic acid solvated with D₂O

Keisuke Hirata^{[a][c][d]}, Kyota Akasaka,^{[a][b]} Otto Dopfer,^{*[d][e]} Shun-ichi Ishiuchi^{*[a][c][d]} and Masaaki Fujii^{*[a][b][d]}

[a] Laboratory for Chemistry and Life Science, Institute of Innovative Research, Tokyo Institute of Technology, 4259 Nagatsuta-cho, Midori-ku, Yokohama, 226-8503, Japan.

[b] School of Life Science and Technology, Tokyo Institute of Technology, 4259 Nagatsuta-cho, Midori-ku, Yokohama, Kanagawa, 226-8503, Japan.

[c] Department of Chemistry, School of Science, Tokyo Institute of Technology, 2-12-1 Ookayama, Meguro-ku, Tokyo 152-8550, Japan.

[d] International Research Frontiers Initiative, Tokyo Institute of Technology, 4259 Nagatsuta-cho, Midori-ku, Yokohama, 226-8503, Japan.

[e] Institut für Optik und Atomare Physik, Technische Universität Berlin, Hardenbergstrasse 36, 10623 Berlin, Germany.

*Corresponding authors

MF: mfujii@res.titech.ac.jp, SI: ishiuchi.s.aa@m.titech.ac.jp, OD: dopfer@physik.tu-berlin.de

ORCID ID

KH: 0000-0003-4472-7992, OD: 0000-0002-9834-4404, SI: 0000-0002-4079-818X, MF: 0000-0003-4858-4618

Experimental.....	3
Complete band assignment in the CAS-IRPD spectra of PABAH ⁺ (D ₂ O) _n (n=5-7).....	4
Figure S1. IRPD spectrum of PABAH ⁺ (D ₂ O) ₅₋₇ in the 2300–2700 cm ⁻¹ range.....	5
Figure S2. IRPD spectrum of singly deuterated (m/z 139) protonated PABA in the 3200–3350 cm ⁻¹ range	6
Figure S3. IRPD spectrum of doubly deuterated (m/z 140) protonated PABA in the 3200–3350 cm ⁻¹ range	7
Figure S4. IRPD spectrum of PABAH ⁺ (D ₂ O) ₆ in the 3400–3600 cm ⁻¹ range.....	8
Figure S5. A schematic of multiply deuterated PABAH ⁺ generated by multiple O→N and N→O proton transfer.	9
Figure S6. IRPD spectra of PABAH ⁺ (H ₂ O) _n (n=5–7) with calculated conformers.	10
References.....	10

Experimental

A detailed description of the cryogenic double ion trap spectrometer is given elsewhere.^{1, 2} A methanol solution of PABA (10^{-5} M, Wako) with 0.5% formic acid was electrosprayed via a glass capillary heated to 80°C to evaporate solvated molecules. The generated ions entered the vacuum setup through an ion funnel. PABAH⁺ ions were mass-selected by a quadrupole mass spectrometer and transported through a tapered hexapole ion guide into a linear octupole ion trap (reaction trap)^{3, 4} maintained at 80 K. Hydrated clusters of PABAH⁺ were generated in the reaction trap by introducing D₂O/He gas via a pulsed valve. H/D exchange reactions seem not to occur in such a trap at $T < 180$ K, as shown in a recent study of protonated glycine.⁵ The hydrated clusters were mass-selected and guided into a second cryogenic quadrupole ion trap (QIT)^{1, 6, 7} kept at 4 K. A mixture of H₂ (20%) and He buffer gas was introduced into QIT and cooled down by collisions with its electrodes. The ions were trapped and cooled to $T \sim 10$ K (vibrational temperature) by collisions with the buffer gas.¹ H₂ molecules were condensed onto the cold ions, forming a variety of weakly-bound H₂-tagged cluster ions. These cluster ions were then irradiated with a focused output of a pulsed and tuneable IR laser (0.7–1.4 mJ/pulse). Absorption of an IR photon triggers the dissociation of the weakly-bound H₂ ligands from the cluster ions, yielding H₂-detached parent ions as photofragments.⁸ The IRPD spectrum of PABAH⁺, which corresponds very closely to its IR absorption spectrum, was measured by monitoring the photofragment signals with a time-of-flight mass spectrometer as a function of IR frequency.

The IR spectra of PABAH⁺(D₂O)_{*n*} were measured by CAS-IRPD spectroscopy⁹ to avoid broadening and congestion of the spectra of the hydrated clusters due to H-bonding and the presence of various hydration isomers. To this end, the hydrated ions were directed into the QIT with high kinetic energy (~ 16 eV) to collisionally dissociate them into bare PABAH⁺ by soft collisions. The dehydrated PABAH⁺ ions generated by this collision-induced dissociation process were H₂-tagged by collisions with cold H₂ gas. The H₂-detached fragments generated upon IR absorption were monitored as a function of the IR frequency to measure the CAS-IRPD spectrum. CAS-IRPD allows to unambiguously determine the protonation site of a molecule by eliminating spectral interferences from solvated molecules and the resulting spectral congestion. Significantly, the protomer population is not changed by the collisional dissociation process due to rapid cooling in the QIT.⁹ To assist the band assignment of the CAS-IRPD spectra (3200–3350 cm⁻¹), the IRPD spectra of N-protomeric PABAH⁺ (m/z 138) and its deuterated isotopologues (m/z 139 and 140) were also measured by changing the ESI solvent from methanol to acetonitrile. Acetonitrile is routinely used to kinetically trap solution-phase stable species (here the N-protomer) in the gas phase.^{10, 11} The mono- and dideuterated isotopologues of PABAH⁺ were generated by seeding acetonitrile with 10% of CH₃OH/CD₃OD (1/1).

Calculated vibrational frequencies of PABAH⁺(H₂)₄ and its isotopologues were obtained from DFT calculations at the \square B97X-D/6-311++G(d,p) level² using Gaussian16.¹² All optimized structures were confirmed to be minima without imaginary vibrational frequencies. The calculated frequencies have been corrected for anharmonicity and deficiencies in the DFT force field using a scaling factor of 0.952.²

Complete band assignment in the CAS-IRPD spectra of PABAH⁺(D₂O)_n (n=5-7)

First, we explain the bands in the 3200–3350 cm⁻¹ range. The bands observed for *n*=5 can be ascribed to the NH stretches of non-deuterated **NH3** and mono-deuterated **NH2D1** except for the band at 3256 cm⁻¹ as described in the manuscript. The band at 3256 cm⁻¹ slightly deviates from $\nu_{NH}^{(N)}$ (3252 cm⁻¹) and is tentatively assigned to a combination band of the O-protomer, as observed in *m/z* 138 (asterisk in Figure 3b in the manuscript). For *n*=6, an additional band at 3251 cm⁻¹ is ascribed to $\nu_{NH}^{(N)}$ of **NH1D2**, indicating the emergence of doubly deuterated **NH1D2**. The NH stretch bands of **NH3** disappear for *n*=7. These observations indicate the deuterated isotopologues observed in the CAS-IRPD spectra: **NH3** and **NH2D1** for *n*=5, **NH3**, **NH2D1**, and **NH1D2** for *n*=6, and **NH2D1** and **NH1D2** for *n*=7. This assignment is further supported by the bands in the ND stretch range (2300–2500 cm⁻¹). The band at 2416 cm⁻¹ observed for *n*=5–7 is assigned to $\nu_{ND}^{(N)}$ of **NH2D1** from the comparison with calculated IR spectra of the deuterated isotopologues of PABAH⁺ (Figure S1). The new bands for *n*=6,7 (2386 cm⁻¹ and the doublet in 2440–2470 cm⁻¹) are assigned to the ND₂ stretches of **NH1D2** (Figure S1). Note that the neutral amino moiety of the O-protomer is partially or fully deuterated for *n*=6,7, indicated by the presence of $\nu_{NH}^{NHD}(O)$ (3486 cm⁻¹), $\nu_{ND}^{NHD}(O)$ (2575 cm⁻¹), and $\nu_{ND_2}^s(O)$ (2501 cm⁻¹) (Figure S1). The multiple deuteration observed for *n*=6,7 is ascribed to H/D exchange reaction by D₂O or the interconversions between N- and O-protomers by O→N and N→O back reactions (Figure S5).

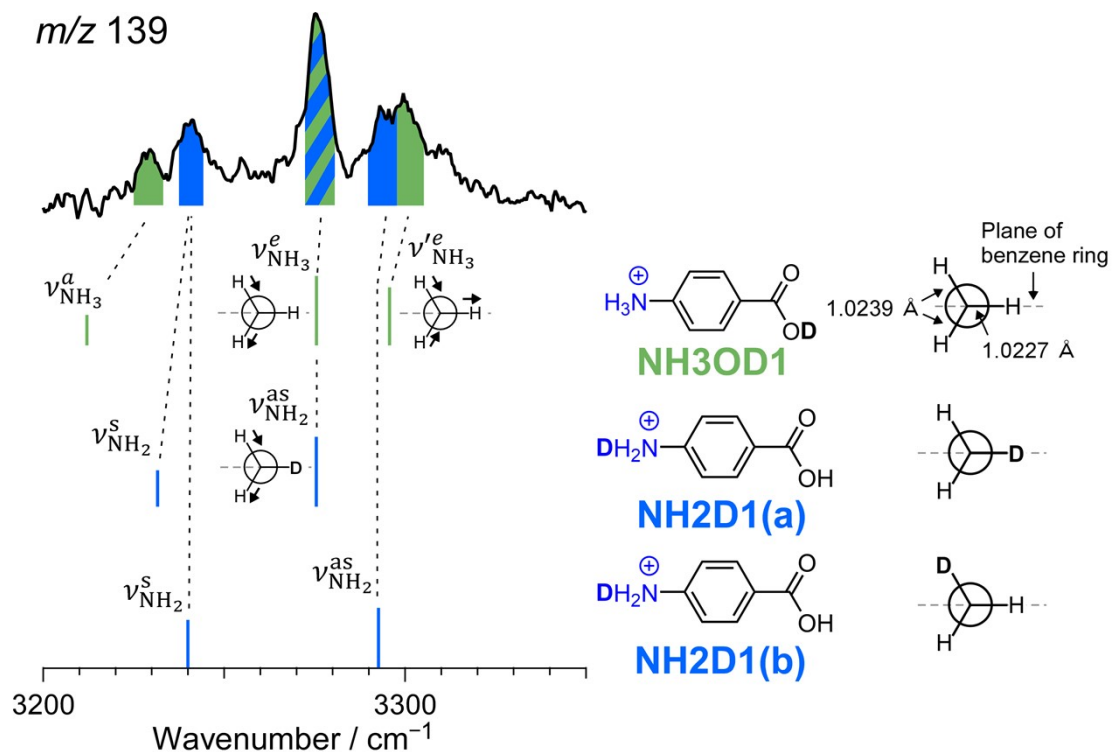


Figure S2. IRPD spectrum of singly deuterated (m/z 139) protonated PABA in the 3200–3350 cm^{-1} range compared to calculated IR spectra of deuterated isotopologues of the N-protomer. The vibrational bands of **NH3OD1** and **NH2D1** are colored in green and blue, respectively. The e -symmetric NH_3 stretch modes of **NH3OD1** are split due to symmetry reduction by the nearby benzene ring. The NH bond in the benzene plane is shorter than the other two NH bonds. The band at 3277 cm^{-1} is assigned to the overlap of $\nu_{\text{NH}_3}^e$ and $\nu_{\text{NH}_2}^{\text{as}}$ due to the similar frequencies and vibrational motions.

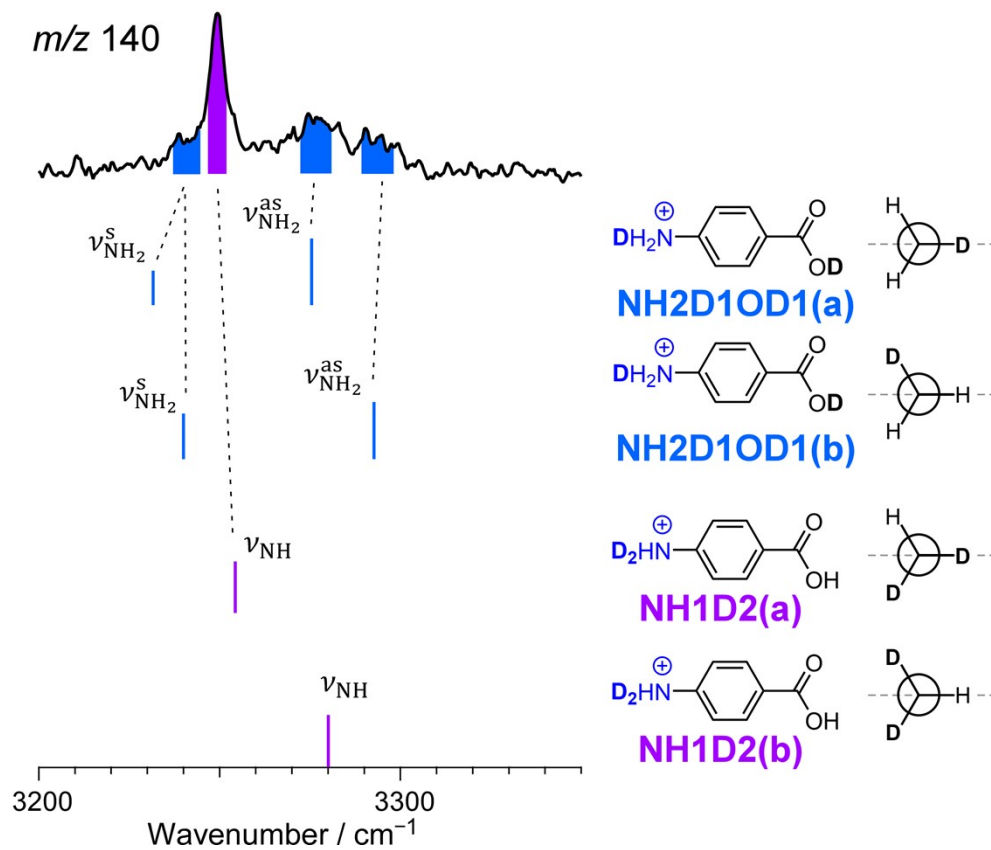


Figure S3. IRPD spectrum of doubly deuterated (m/z 140) protonated PABA in the 3200–3350 cm^{-1} range compared to calculated IR spectra of deuterated isotopologues of the N-protomer. The vibrational bands of **NH2D1OD1** and **NH1D2** are colored in blue and purple, respectively. Note that the band at 3277 cm^{-1} may be overlapped with ν_{NH} of **NH1D2(b)**.

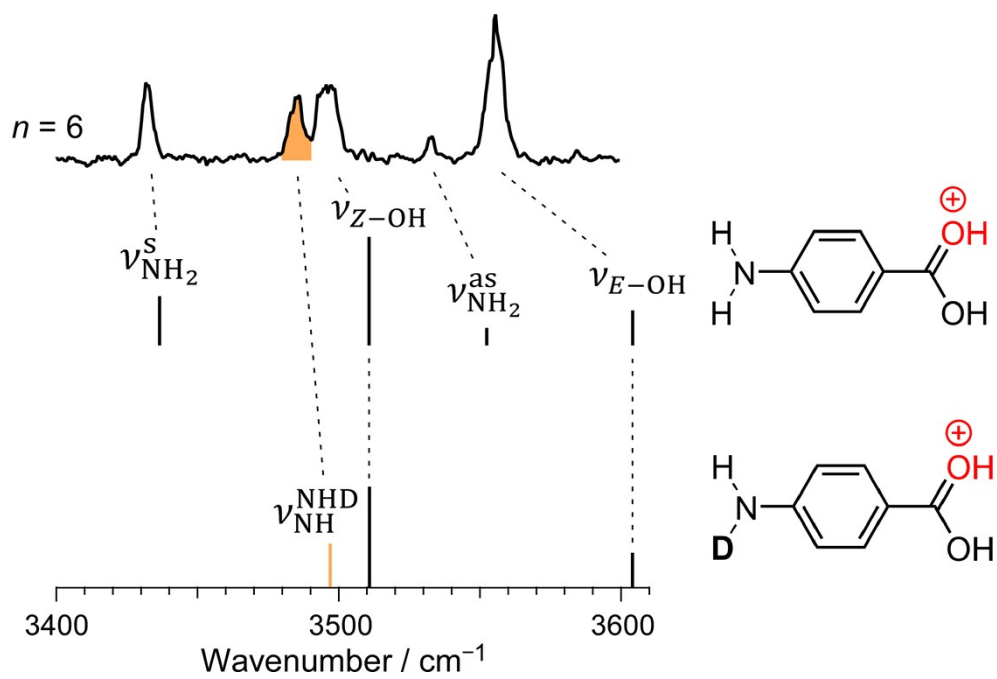


Figure S4. IRPD spectrum of PABAH⁺(D₂O)₆ in the 3400–3600 cm⁻¹ range compared to calculated IR spectra of the O-protomer and its isotopologue. The vibrational band ν_{NH}^{NHD} is colored in orange.

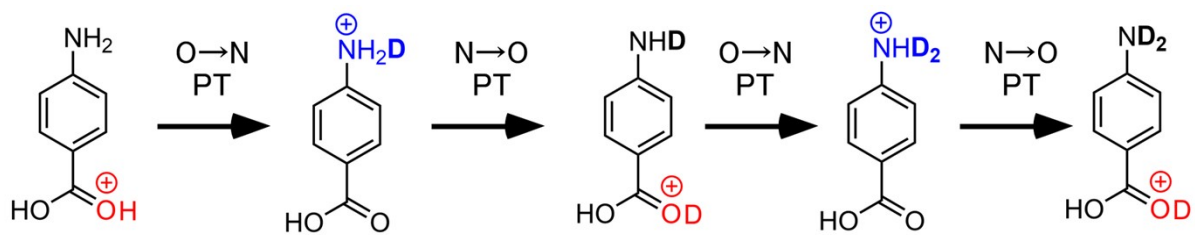


Figure S5. A schematic of multiply deuterated PABA H^+ generated by multiple $\text{O} \rightarrow \text{N}$ and $\text{N} \rightarrow \text{O}$ proton transfer (PT).

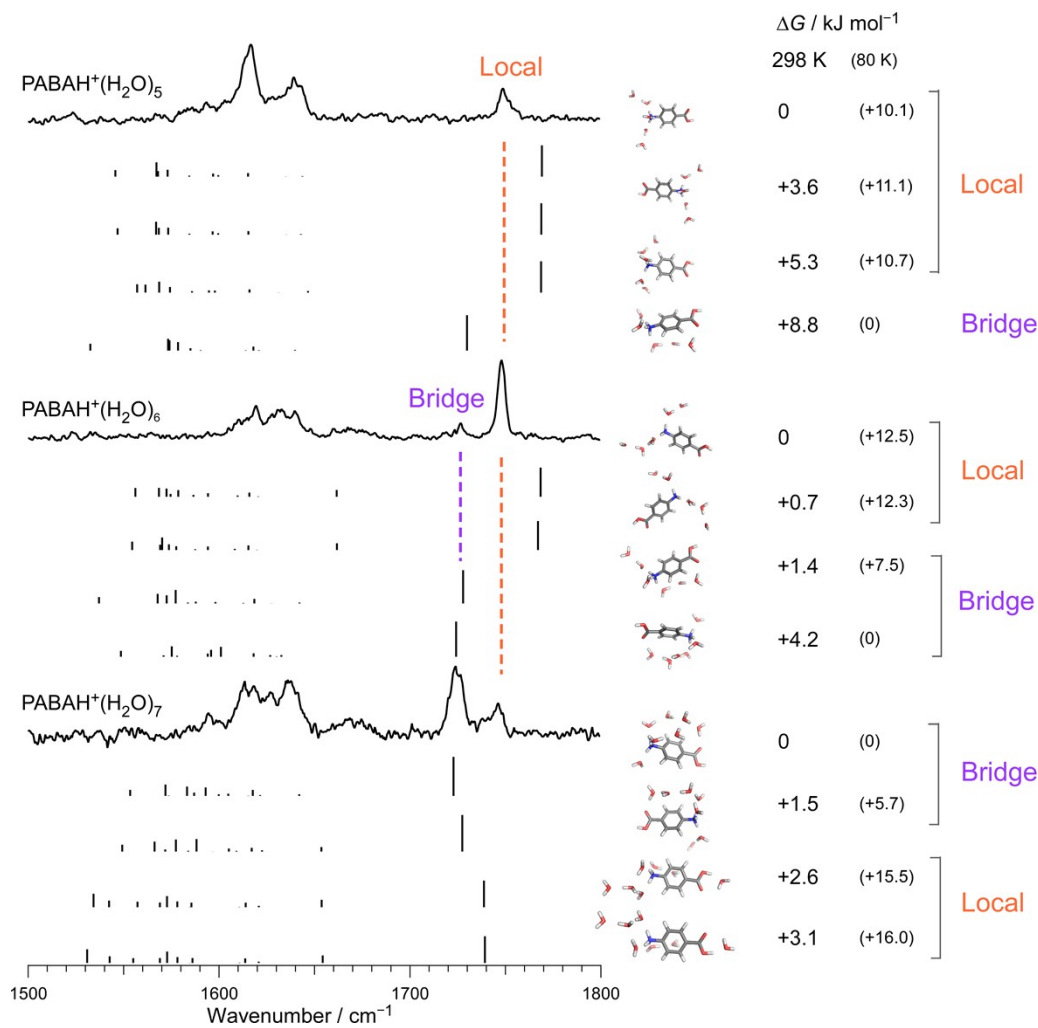


Figure S6. IRPD spectra of PABAH⁺(H₂O)_n ($n=5-7$)² with calculated conformers. The calculated conformers are divided into local and bridge groups: local structures take a conformation in which water only hydrates the charged amino site, while the bridge structure has a H-bonded water bridge between the N and O sites. The Gibbs free energy (ΔG) for each conformer is given at both 80 and 298 K with respect to the most stable N-protomer.

References

1. S. Ishiuchi, H. Wako, D. Kato and M. Fujii, *J. Mol. Spectrosc.*, 2017, **332**, 45-51.
2. K. Akasaka, K. Hirata, F. Haddad, O. Dopfer, S. Ishiuchi and M. Fujii, *Phys. Chem. Chem. Phys.*, 2023, **25**, 4481-4488.
3. B. M. Marsh, J. M. Voss and E. Garand, *J. Chem. Phys.*, 2015, **143**, 204201.

4. E. Sato, K. Hirata, J. M. Lisy, S. Ishiuchi and M. Fujii, *J. Phys. Chem. Lett.*, 2021, **12**, 1754-1758.
5. J. M. Voss, K. C. Fischer and E. Garand, *J. Phys. Chem. Lett.*, 2018, **9**, 2246-2250.
6. O. V. Boyarkin, S. R. Mercier, A. Kamariotis and T. R. Rizzo, *J. Am. Chem. Soc.*, 2006, **128**, 2816-2817.
7. J. G. Redwine, Z. A. Davis, N. L. Burke, R. A. Oglesbee, S. A. McLuckey and T. S. Zwier, *Int. J. Mass Spectrom.*, 2013, **348**, 9-14.
8. M. Z. Kamrath, E. Garand, P. A. Jordan, C. M. Leavitt, A. B. Wolk, M. J. Van Stipdonk, S. J. Miller and M. A. Johnson, *J. Am. Chem. Soc.*, 2011, **133**, 6440-6448.
9. K. Hirata, F. Haddad, O. Dopfer, S. Ishiuchi and M. Fujii, *Phys. Chem. Chem. Phys.*, 2022, **24**, 5774-5779.
10. S. Warnke, J. Seo, J. Boschmans, F. Sobott, J. H. Scrivens, C. Bleiholder, M. T. Bowers, S. Gewinner, W. Schöllkopf, K. Pagel, et al., *J. Am. Chem. Soc.*, 2015, **137**, 4236-4242.
11. T. Khuu, N. Yang and M. A. Johnson, *Int. J. Mass Spectrom.*, 2020, **457**, 116427.
12. M. Frisch, G. Trucks, H. Schlegel, G. Scuseria, M. Robb, J. Cheeseman, G. Scalmani, V. Barone, G. Petersson, H. Nakatsuji, et al., Gaussian, Inc. Wallingford, CT2016.